Neoadjuvant Intravenous Oncolytic Vaccinia Virus Therapy Promotes Anticancer Immunity in Patients

Adel Samson[1], Emma J. West[1], Jonathan Carmichael[1], Karen J. Scott[1], Samantha Turnbull[1], Bethany Kuszlewicz[1], Rajiv V. Dave[2], Adam Peckham-Cooper[3], Emma Tidswell[1], Jennifer Kingston[3], Michelle Johnpulle[3], Barbara da Silva[1], Victoria A. Jennings[1], Kaidre Bendjama[4], Nicolas Stojkowitz[4], Monika Lusky[4], K.R. Prasad[3], Giles J. Toogood[3], Rebecca Auer[5], John Bell[5], Chris J. Twelves[1], Kevin J. Harrington[6], Richard G. Vile[7], Hardev Pandha[8], Fiona Errington-Mais[1], Christy Ralph[1], Darren J. Newton[1], Alan Anthoney[1], Alan A. Melcher[6], and Fiona Collinson[1]

ABSTRACT

Improving the chances of curing patients with cancer who have had surgery to remove metastatic sites of disease is a priority area for cancer research. *Pexa-Vec* (*Pexastimogene Devacirepvec*; JX-594, TG6006) is a principally immunotherapeutic oncolytic virus that has reached late-phase clinical trials. We report the results of a single-center, nonrandomized biological end point study (trial registration: EudraCT number 2012-000704-15), which builds on the success of the presurgical intravenous delivery of oncolytic viruses to tumors. Nine patients with either colorectal cancer liver metastases or metastatic melanoma were treated with a single intravenous infusion of *Pexa-Vec* ahead of planned surgical resection of the metastases. Grade 3 and 4 *Pexa-Vec*–associated side effects were lymphopaenia and neutropaenia. *Pexa-Vec* was peripherally carried in plasma and was not associated with peripheral blood mononuclear cells. Upon surgical resection, *Pexa-Vec* was found in the majority of analyzed tumors. *Pexa-Vec* therapy associated with IFNα secretion, chemokine induction, and resulted in transient innate and long-lived adaptive anticancer immunity. In the 2 patients with significant and complete tumor necrosis, a reduction in the peripheral T-cell receptor diversity was observed at the time of surgery. These results support the development of presurgical oncolytic vaccinia virus-based therapies to stimulate anticancer immunity and increase the chances to cure patients with cancer.

Introduction

Patients with advanced solid malignancies can undergo surgical resection of their metastatic disease with curative intent. However, only a minority of these patients remain cancer-free long term, due to either incomplete tumor resection or the presence of micrometastatic disease at the time of surgery. For patients with colorectal liver metastases (CRLM), survival at 5 years following liver resection is approximately 50%, despite the availability of combination perioperative chemotherapy (1). Likewise, approximately 60% of patients with melanoma that has spread to lymph nodes can relapse following surgical resection and adjuvant treatment (2). For these patients, effective novel systemic therapies administered prior to (neoadjuvant therapy), or shortly after surgery (adjuvant therapy), hold the potential to significantly enhance the chances of tumor clearance.

Oncolytic viruses (OV) are principally immunotherapeutic viruses that preferentially replicate in malignant cells, thereby inducing immunogenic cell death. Several engineered viruses have reached randomized studies, with three agents currently licensed for standard care (3). One of the most clinically tested oncolytic viruses, *Pexa-Vec* (*Pexastimogene Devacirepvec*; JX-594, TG6006), is an engineered Wyeth-strain vaccinia virus (4) under development by Transgene (5) and SillaJen (6). *Pexa-Vec* tumor specificity is enhanced by deletion of thymidine kinase, an enzyme of the DNA precursor pathway, which is strictly regulated during the normal cellular cycle, but highly expressed in growing malignant cells (7). *Pexa-Vec* also expresses GMCSF, which promotes antitumor immunity by inducing proliferation and differentiation of myeloid precursors, alongside the stimulation, recruitment, and maturation of dendritic cells (DC; refs. 8, 9). Clinical and *in vitro* studies have helped to elucidate the fundamental mechanisms of *Pexa-Vec* therapy, namely tumor-specific virus replication, expression of GMCSF, and the stimulation of CTL tumor infiltration (10). Other mechanisms of therapy include antibody-mediated, complement-dependent cancer cell cytotoxicity (11) and *Pexa-Vec* replication in tumor-associated endothelial cells, leading to disruption of tumor blood flow, hypoxia, and necrosis (12).

Pexa-Vec has shown promising clinical signs of efficacy as a single agent, including in a randomized study between low-dose (1×10^8 plaque-forming units; p.f.u) and high-dose (1×10^9 p.f.u) intratumoural injection in patients with hepatocellular carcinoma, where overall survival was significantly longer for patients in the high-dose group (14.1 vs. 6.7 months; ref. 13). Furthermore, intravenous delivery of *Pexa-Vec* to tumors, a critical feature for the treatment of micrometastatic disease, is achievable using a dose of 1×10^9 p.f.u (14).

[1]Leeds Institute of Medical Research at St. James's, University of Leeds, Leeds, United Kingdom. [2]Manchester University NHS Foundation Trust, Manchester, United Kingdom. [3]Leeds Teaching Hospitals NHS Trust, Leeds, United Kingdom. [4]Transgene, Strasbourg, France. [5]Ontario Health Research Institute, Ottawa, Canada. [6]The Institute of Cancer Research, London, United Kingdom. [7]Mayo Clinic, Rochester, Minnesota. [8]University of Surrey, Guildford, United Kingdom.

Therefore, we sought to clinically develop intravenous *Pexa-Vec* delivery as a neoadjuvant, multimechanistic therapy for patients with metastatic solid malignancies. Herein, we showed in 9 patients that the administration of a single intravenous infusion of *Pexa-Vec* ahead of planned surgical resection of advanced CRLM or metastatic melanoma, resulted in acceptable patient safety and pathologic evidence of tumor necrosis. *Pexa-Vec* associated with the plasma compartment of peripheral blood, resulting in delivery of virus to tumor and promotion of innate anticancer immunity. Furthermore, a single neoadjuvant infusion of *Pexa-Vec* stimulated long-lived T-cell anticancer immune responses, with repertoire sequencing suggesting that pathologic tumor response associated with a perceived reduction in global T-cell diversity. These results support the continued development of *Pexa-Vec* and other OVs as perisurgical treatments, to increase the probability of tumor clearance.

Materials and Methods

Availability of data and material

All data and materials are available by request from the corresponding author.

Ethics approval and consent to participate

The study was approved by the National Research Ethics Service (NRES) Committee London—West London and the Gene Therapy Advisory Committee (GTAC) approval number 101521. All patients granted explicit written consent for clinical trial participation.

Experimental design

The trial, EudraCT (number 2012-000704-15) was open between September 2015 and June 2018 in accordance with Declaration of Helsinki ethical guidelines. This was an open-label, nonrandomized study of *Pexa-Vec* given as a 1-hour intravenous infusion to patients prior to planned surgical resection of tumor. The trial inclusion and exclusion criteria were as follows:

Inclusion criteria

(i) Patients with histologically proven or radiological findings consistent with locally advanced/poor prognosis or metastatic cancer, planned for surgical resection (curative or palliative) of primary or metastatic disease as part of standard clinical care. Patients with the following diseases were eligible: (a) metastatic melanoma due for lymph node dissection for lymph node macrometastases (stage IIIB/C) or metastasectomy at any other site; (b) muscle-invasive transitional cell bladder cancer suitable for surgical resection, that is, partial or total cystectomy; (c) primary hepatocellular carcinoma, planned for liver resection; (d) colorectal cancer with liver metastases planned for metastasectomy or liver resection; (e) locally advanced/metastatic renal cell cancer planned for palliative nephrectomy. (ii) Patients were willing to have full preoperative work-up prior to planned resection, consistent with standard clinical practice appropriate for the disease site/surgical intervention, (iii) were fit for the planned surgical intervention, (iv) had a life expectancy of at least 3 months, (v) were at least 18 years of age, (vi) had an Eastern Cooperative Oncology Group performance status score 0–2, (vii) hemoglobin $\geq$ 9 g/dL (correction with transfusion allowed), (viii) platelets $\geq$ 100 $\times$ 109 (without platelet transfusion), (ix) absolute neutrophil count $\geq 1.5 \times 10^9$/L, (x) total bilirubin $\leq 1.5 \times$ upper limit of normal (ULN), (xi) aspartate aminotransferase and/or alanine aminotransferase $\leq 2.5 \times$ ULN, (xii) INR ≤ 1.7, and (xiii) serum creatinine $\leq 1.5 \times$ ULN. (xiv) For patients who are sexually active, able,

and willing to abstain from sex for 3 weeks and then use a barrier method of contraception for a further 3 weeks after the JX-594 treatment. A negative pregnancy test was required within 24 hours of treatment if patients were a female of child-bearing potential. (xv) Patients were willing and able to provide informed consent and willing and able to comply with scheduled visits, the treatment plan, and laboratory tests.

Exclusion criteria

Patients who: (i) were pregnant or breast-feeding an infant, (ii) were on antiviral therapy, immunotherapy, had known HIV infection or hepatitis B/C, (iii) had clinically significant active infection or uncontrolled medical condition (e.g., pulmonary, neurological, cardiovascular, gastrointestinal, genitourinary), such that the patient was unfit for surgery or results interfered with interpretation of the trial, (iv) had known CNS malignancy (including history of brain metastases completely resected or treated by gamma knife therapy or whole brain radiotherapy), (v) had clinically significant and reaccumulating ascites, pericardial and/or pleural effusions, (vi) had tumor(s) in a location that would potentially result in significant clinical adverse effects if post-treatment tumor swelling were to occur (e.g., tumors causing near total blockage of the common bile duct), and (vii) received anticancer therapy (e.g., chemotherapy, surgery, radiotherapy, investigational agent) within 4 weeks prior to treatment. Patients were also excluded if: (viii) they experienced a severe systemic reaction or side effect as a result of a previous smallpox vaccination (previous smallpox vaccination is not required), (ix) had a history of exfoliative skin condition (e.g., eczema or ectopic dermatitis) requiring systemic therapy, (x) used of IFN/pegylated IFN or ribavirin that could not be discontinued within 14 days prior to any JX-594 dose, (xi) had active cardiovascular disease, including but not limited to significant coronary artery disease (e.g., requiring angioplasty or stenting) or congestive heart failure within the preceding 12 months (the potential risk of hypotension after administration of JX-594 in conjunction with any underlying cardiac disease should be taken into consideration), (xii) inability to suspend treatment with antihypertensive medication if necessary (including but not limited to: diuretics, beta-blockers, angiotensin converting enzyme inhibitors, aldosterone antagonists, etc.) for 48 hours prior to and 48 hours after JX-594 treatment, (xiii) pulse oximetry O_2 saturation less than 90% at rest on room air, and (xiv) previous treatment with JX-594 or other vaccinia vector–based treatment.

A total of 9 patients each received a single dose of 1×10^9 p.f.u. *Pexa-Vec* via intravenous infusion 10 to 22 days prior to surgery at St. James's University Hospital (SJUH), Leeds, United Kingdom. Three patients had metastatic melanoma and 6 had CRLM. Eight patients completed their planned surgery, and 1 patient (patient 07) had surgery cancelled when an up-to-date CT scan revealed pulmonary metastases. The primary end point of the study was the presence of *Pexa-Vec* in resected tumor tissue and blood. All patients gave written, informed consent according to good clinical practice guidelines. Protocol, patient information sheet, and consent forms were approved by the United Kingdom Medicines and Healthcare products Regulatory Authority, regional ethics review committee, as well as institutional review at SJUH. The trial management committee met on a monthly basis to discuss study progress, including patient safety and adverse events.

Pexa-Vec

Pexa-Vec (*Pexastimogene Devacirepvec*; JX-594, TG6006), a replication-competent, transgene-armed therapeutic vaccinia virus, and *Pexa-Vec*-GFP were provided by Transgene S.A, France. *Pexa-Vec* is engineered for viral thymidine kinase gene inactivation and expression

of GMCSF and β-galactosidase transgenes under the control of the synthetic early-late and p7.5 promoters, respectively. *Pexa-Vec* was stored at 1×10^9/mL at $-80°C$ for use in *in vitro* experiments.

Patient samples

Blood and tissue samples (metastatic lesions or lymph nodes, where applicable) were collected, processed, and analyzed using the Translational Cancer Immunotherapy Team quality-assured lab manual, which included SOPs to standardize all processes. Peripheral blood was collected into K_3EDTA and serum clot activator vacuette tubes (both Greiner) and processed within 2 hours of venepuncture. Blood samples were taken on day 1 (pre- and 1-hour postinfusion), day 2, day 3 (optional), day 5 (optional), on the day of surgery, 1-month postsurgery, and 3 months postsurgery. Tumor (and corresponding normal margins, if available) were taken from planned surgical resections.

Isolation of peripheral blood mononuclear cells, plasma, and serum from peripheral blood

All blood processing steps were performed at ambient temperature or at a controlled temperature of 20°C during centrifuge spins.

Plasma

K_3EDTA blood was centrifuged for 10 minutes at $2,000 \times g$ and plasma was harvested from the resulting upper layer. Aliquots were stored at $-80°C$.

Peripheral blood mononuclear cells

Peripheral blood mononuclear cells (PBMC) were isolated from K_3EDTA blood by density-gradient separation over lymphoprep (Stemcell Technologies) as per manufacturer's instructions. Cells were frozen at 1×10^7/mL in 40% [volume for volume (v/v)] RPMI1640 (Sigma) containing 5 mmol/L L-glutamine (Sigma), 1 mmol/L sodium pyruvate (Sigma), 50% (v/v) pooled human serum (HS; BioIVT), and 10% (v/v) dimethyl sulphoxide (DMSO; Sigma). Where cultured, PBMCs were placed in RPMI containing 5 mmol/L L-glutamine and supplemented with 10% (v/v) FCS (Invitrogen). PBMCs were stored in liquid nitrogen.

Serum

Blood collected in clot activator tubes was left to clot for a minimum of 30 minutes post-venepuncture and then centrifuged at $2,000 \times g$ for 10 minutes. Serum was harvested from the resulting upper layer. Aliquots were stored at $-80°C$.

Full blood counts

Full blood counts were performed, where appropriate, at SJUH as part of standard clinical care. The Patient Pathway Manager and Results Server systems (Leeds Teaching Hospitals Trust in-house electronic health record system for West Yorkshire and Humber region, United Kingdom) were used to acquire total lymphocyte counts (expressed as 10^9/L) throughout treatment. Normal ranges of lymphocytes were defined by SJUH as $1–4.5 \times 10^9$/L.

IHC

IHC was performed on formalin-fixed paraffin-embedded tissue obtained from surgical resection of patient tumors or lymph nodes. Tissue for IHC was processed using an automated Bond Max system (Leica Biosystems) as described in ref. 15. IHC for *Pexa-Vec* was performed by Histalim (France) following company validated protocols using 1:200 dilution of polyclonal rabbit-anti-vaccinia virus antibody (Meridian Life Sciences; RRID: AB_153134). Mouse anti-

human CD8 antibody (Dako; RRID: AB_2075537) was used at 1:100 dilution, followed by anti-mouse secondary (Abcam; RRID: AB_10680417) at 1:500. CD8 positivity was detected using the ImmPACT 3,3′-Diaminobenzidine horseradish peroxidase (HRP) Substrate Kit (Vector Labs; RRID: AB_2336520) or ImmPACT Vector Red (Vector Labs; RRID: AB_2336524). Antibodies against tumor-associated antigens (TAA) were used as follows: anti-human carcinoembryonic antigen (CEA; RRID: AB_304463) at 5 μg/mL, anti-human Melan-A (RRID: AB_305836) at 1:50 dilution, both with an anti-mouse secondary antibody at 1:2,000 dilution (all Abcam). Enzymatic detection was performed using ImmPACT VIP for the melanoma (Melan-A) tissue and ImmPACT DAB HRP Substrate Kit (RRID: AB_ 2336520) for the CRLM (CEA) tissue (both Vector Labs). Finally, rabbit anti-human PD-1 (1:200; Abcam; RRID: AB-230_881954) and mouse anti-human Ki67 (1:75; Dako; RRID: AB_2142367) were detected with the ImmPACT VIP HRP or DAB Peroxidase Substrate kits. Control sections were processed as above, without the addition of primary antibody. Hematoxylin and eosin (H&E; both Sigma) staining was performed on all patient tissue sections. Digital images were acquired using an Aperio AT2 Scanscope (Leica Biosytems) at ×20 magnification and quantified using ImageScope software (RRID: SCR_014311).

qPCR

qPCR was performed using DNA extracted from PBMCs and plasma using a DNeasy Blood and Tissue Kit and a Circulating Nucleic Acid kit, respectively (Qiagen). Primers corresponding to the vaccinia E3 L gene (forward: 3′-TCCGTCGATGTCTACACAGG-5′ and reverse: 5′-ATGTATCCCGCGAAAAATCA-3′) (Integrated DNA Technologies) were used to detect the presence of *Pexa-Vec* (five replicates), alongside a standard curve of known *Pexa-Vec* DNA concentration (three replicates) and a control gene (18s; 3 replicates; Qiagen), on an Applied Biosystems QuantStudio 5 Real-Time PCR System (Thermo Fisher Scientific) using SYBR green detection method (Thermo Fisher Scientific). 2 μL DNA was included in the reaction mix, which equated to a range of 100–200 ng/μL total DNA. PCR data were analyzed using a QuantStudio three-dimensional AnalysisSuite Cloud (Thermo Fisher Scientific).

Cell culture

The African monkey green kidney cell line (Vero), a melanoma cell line (Mel888) and a colorectal cell line (SW620; all ATCC) were maintained in full growth medium: DMEM (Sigma) containing 5 mmol/L L-glutamine and supplemented with 10% (v/v) FCS for approximately 2 weeks before use. Cells were routinely tested and found to be negative for *Mycoplasma* infection. Cell lines were authenticated by short tandem repeat profiling.

Neutralizing antibodies

Neutralizing antibodies (NAb) were detected using a modified serial dilution assay of heat-inactivated (HI) patient serum as described previously (16). Briefly, 3-fold serial dilutions (1:3 to 1:531,441) of HI-serum samples were incubated with *Pexa-Vec*. After incubation for 3 hours at 37°C, the diluted HI-serum samples were transferred onto monolayers of Vero cells resulting in a final virus dose of 50 p.f.u./cell. Cells alone or with *Pexa-Vec* dilution only were also cultured as negative and positive controls, respectively. After a further 72 hours of incubation, MTT (5 mg/mL; Sigma) was added to each well and left for 4 hours, before the removal of all medium and addition of 150 μL DMSO (Thermo Fisher Scientific) to each well. Absorbance of samples was then read at 540 nm on a Thermo Multiskan EX plate reader

(Thermo Fisher Scientific). NAb titers were calculated as 1/end point, which equates to the last serum dilution at which no antibody neutralization of *Pexa-Vec*–induced killing was observed ($n = 9$). Data are shown as mean + SEM.

Luminex

Bio-Plex Pro Cytokine and Chemokine Assays (21-plex; human group I and 27-plex; human group II or 48-plex; human cytokine; both Bio-Rad) were used to determine concentration of soluble mediators in patient plasma samples throughout treatment, as per manufacturer's instructions. Plasma was diluted 2-fold and 50 μL loaded per well in duplicate. Bio-Plex plates were analyzed using the Bio-Plex 200 system and the Bio-Plex Manager 6.1 for data acquisition and analysis (Bio-Rad). IFNβ was measured in samples using the VeriKine-HS Human Interferon Beta ELISA Kit for plasma (R&D Systems), as per manufacturer's instructions and plates were analyzed using a Thermo Multiskan EX plate reader. Standard curves included within each kit were used to calculate the concentration of each solute in patient plasma based on emission or absorbance spectra, as appropriate to the kit. Data are expressed as mean ± SEM relative fold change in posttreatment samples compared with pretreatment samples. Statistical significance between time points was determined using paired *t* tests; *, $P < 0.05$; **, $P < 0.01$ ($n = 9$).

Natural killer–cell degranulation assays using patient PBMCs

PBMCs from specified time points prior to (D1 pre) and following *Pexa-Vec* infusion were cocultured at a ratio of 1:1 with Mel888 or SW620 tumor cells for patients with melanoma and CRLM, respectively, for 1 hour, and then 1 μL/mL brefeldin (Sigma) was added. Coculture continued for a further 4 hours before PBMCs were harvested, washed, and stained for anti-CD3-PerCP (5 μL; SK7; BD Biosciences), anti-CD56-PE (2 μL; AF12-7H3; Miltenyi Biotec), and anti-CD107a/b-FITC (5 μL; H4A3; BD Biosciences) for 30 minutes at 4°C. PBMCs were washed and fixed in 1% PFA. CD107 positivity was assessed using a CytoFLEX S flow cytometer and analysis was performed using CytExpert software (RRID: SCR_017217; both Beckman Coulter). Data are expressed as mean ± SEM% positive CD107 staining on NK cells (CD3$^-$ CD56$^+$). Statistical significance was determined by paired *t* tests (*, $P < 0.05$; $n = 9$).

Natural killer cell CD69 expression

Assessment of natural killer (NK)-cell CD69 expression was performed using flow cytometry either: (i) as described above using anti-CD69-APC (5 μL; Miltenyi Biotec, RRID: AB_2784271) or (ii) using a panel of custom-designed DURAClone tubes (Beckman Coulter) incorporating CD3 (UCHT1; Pacific Blue), CD56 (N901; PC7) and CD69 (TP.55.3; APC). Data were acquired on a CytoFLEX S flow cytometer, and analysis was performed using CytExpert software. Data are expressed as mean ± SEM % positive CD69 staining on NK cells. Statistical significance was determined by paired *t* tests (*, $P < 0.05$; $n = 9$).

mRNA expression analysis of patient PBMCs

PBMC RNA was isolated using an RNeasy Plus Mini kit (Qiagen) following manufacturer's instructions. Analysis was performed using the HTG EdgeSeq Precision Immuno-Oncology Panel by HTG Molecular, Arizona, which contains probes for 1,410 genes. The quantitative nuclease protection assay was used to ensure robust RNA quality to a minimum of 50 bases. All sequencing was performed on the Illumina NextSeq. Differential expression analysis was performed using the

DESeq2 package (version 1.14.1; Bioconductor; RRID: SCR_006442), utilizing median data normalization. A read depth of 14 million to 10,000 was used as a threshold. Data are expressed as $\log_2$ (CPM) for the average expression of each probe across all groups after normalization. Statistical significance between time points is shown by an adjusted *P* value (P_{adj}); *, $P < 0.05$; **, $P < 0.01$; ***, $P < 0.001$; ****, $P < 0.0001$ ($n = 7$). Reagents listed in Supplementary Data S1.

Enzyme-linked immunosorbent spot assays

Briefly, 1×10^5 patient PBMCs were incubated per well in the presence of either 2 μg/mL CEA or melanoma antigen recognized by T cells-1 (MART-1) overlapping peptide pools, or with 2 μg/mL CEF peptide pool (positive control; all Cambridge Biosciences). Media alone (negative control) and 10 p.f.u/cell *Pexa-Vec* were also used. IFNγ secretion from activated T cells was detected using a matched paired antibody kit (MabTech) and spot-forming units (SFU) were visualized using BCIP/NBT substrate (MabTech). Images were captured using an AID enzyme-linked immunosorbent spot (ELISpot) reader (AID GmbH). Data are presented as mean SFU per well (in triplicate) + SEM. Statistical significance between time points was determined by fitting a mixed model for one-tailed multiple comparisons; *, $P_{adj} < 0.05$ ($n = 3$–9, dependent on sample availability).

Pexa-Vec peripheral blood carriage

Peripheral blood from healthy donors (HD) was incubated with 2×10^5 p.f.u/mL *Pexa-Vec in vitro* for 1 hour at room temperature. Blood was processed to isolate PBMCs and plasma before DNA was extracted, and qPCR was performed to quantify *Pexa-Vec* DNA, as described above. A standard curve of known *Pexa-Vec* DNA was used to estimate the concentration of *Pexa-Vec* DNA in PBMCs and plasma. Data are shown as mean + SEM ng DNA per 5 mL initial blood volume ($n = 5$ replicates) for three donors. Statistical significance was determined by paired *t* tests; **, $P < 0.01$; ***, $P < 0.001$.

TCRB sequencing

DNA was extracted using an AllPrep RNA/DNA mini kit (Qiagen) following manufacturer's instructions. *TCRB* was amplified from genomic DNA, extracted from patient samples, using a modified version of the BIOMED-2 sequencing protocol (17). Modifications included the generation of amplicons using Phusion High-fidelity Master Mix (Thermo Fisher Scientific) with an annealing temperature of 63°C, with a final magnesium concentration of 3.5 mmol/L. Adapters attached to the PCR primers (Supplementary Data S2) allowed sequences to be indexed using the Nextera XT indexing kit (Illumina) for sample multiplexing. Libraries were sequenced on a single lane of an Illumina MiSeq by the Leeds University sequencing facility using a 2 × 300 bp kit. The quality of demultiplexed reads was assessed by fastqc (18), and reads were trimmed to remove adapters and low-quality bases using trimmomatic (19) and trim galore (20). High-quality reads (Phred>30) were then overlapped with FLASH (21) and aligned to the IMGT database using MiXCR (22), which discarded erroneous and nonproductive rearrangements. Clones were defined by having the same TCRBV/J segment and identical CDR3 sequence, and their abundance was adjusted using the absolute T-cell count to eliminate amplification errors. For generation of inverse Simpson indices, assessment of antigen specificities and generation of Circos (RRID: SCR_011798) plots, the subsequent output was filtered into VDJTools (23) and processed in R (24) using Immunarch (25), circlize (26), and ggplot2 (27). Statistical analysis of the percent change

in T-cell diversity at the time of surgery was performed using a one-tailed Mann–Whitney test, *, $P < 0.05$.

PBMC viability assay

HD PBMCs were isolated from leukocyte apheresis cones supplied by the National Health Service Blood and Transplant unit (United Kingdom) and treated with 0.1 p.f.u./cell *Pexa-Vec* for 72 hours. Viability of PBMC populations were assessed by staining, as described above, with 5 μL anti-CD3-PerCP (CD3$^+$ T cells), 2 μL anti-CD56-APC (CD3$^-$CD56$^+$ NK cells; REA196, Miltenyi Biotec), 5 μL anti-CD19-FITC (CD19$^+$ B cells) (SJ25C1, BD Biosciences), 20 μL anti-CD14-PE (CD14$^+$ monocytes; M5E2, BD Biosciences), and Zombie UV fixable viability kit (BioLegend) following manufacturer's instructions. Flow cytometry analysis was performed using a CytoFLEX S and CytExpert software.

Immunofluorescence to detect tumor-specific replication of *Pexa-Vec*

Liver metastases and accompanying background liver were obtained from freshly resected liver specimens immediately following surgical resection from 10 patients with CRLM undergoing planned surgical resection of liver metastases but not participating in the trial. Written, informed consent was obtained in accordance with institutional ethics review and approval. Tissue cores were made using a Tru-Cut biopsy needle (CareFusion), resulting in cores of 1 mm diameter and 15 mm length, and cores were subsequently divided into three 5-mm-length cores. Tissue cores were analyzed as soon as possible following resection and treated with 1×10^7 p.f.u. *Pexa-Vec*-GFP or PBS for 96 hours. Prior to image acquisition, 4′,6-diamidino-2-phenylindole staining was performed following cell penetration with 0.1% Triton X (both Sigma). High-resolution images were taken using a Nikon A1 Confocal Laser Scanning Microscope (Nikon).

In vitro NK-cell activation

HD PBMCs were treated with *Pexa-Vec* for 24 hours with or without (±) type I IFNα/β blockade or monocyte depletion. For type I IFN neutralization, PBMCs were preincubated for 30 minutes with polyclonal antibodies to IFNα, IFNβ (both anti-sheep), and IFNα/β receptor chain 2 (anti-mouse; all PBL Assay Science) or isotype control (anti-sheep, Sigma; and anti-mouse, R&D Systems) prior to addition of 1 p.f.u./cell *Pexa-Vec* for 24 hours as described previously (28). For monocyte depletion, CD14$^+$ cells were depleted from whole PBMCs using CD14-positive magnetic bead selection on LS MACS columns (Miltenyi Biotec), according to the manufacturer's instructions. The CD14-depleted PBMCs were at least 97% pure of CD14$^+$ cells. After virus treatment for 24 hours, NK-cell CD69 expression and CD107 degranulation (as described above) were determined using an Attune NxT Acoustic Focusing Cytometer (Life Technologies), and data were analyzed using Attune Cytometric Software (v2.1.0; Life Technologies). For NK-cell CD107 degranulation, PBMCs (±1 p.f.u. *Pexa-Vec*) were cocultured with SW620 cells at 10:1 effector:target ratio, following the same protocol as previously described for the patient CD107 assay.

Data availability statement

Raw data for mRNA expression analysis were generated at HTG Molecular. Derived data supporting the findings of this study are available from the corresponding author upon request. The TCRB sequencing data generated in this study are publicly available in NCBI; BioProject accession number PRJNA825493.

Results

Clinical outcomes

We recruited 9 patients (3 patients with metastatic melanoma and 6 patients with CRLM) to a phase Ib window-of-opportunity trial. Each patient received a single, 1-hour intravenous infusion of 1×10^9 p.f.u. *Pexa-Vec*, 14 (±4) days ahead of planned surgical resection of metastatic melanoma or CRLM (**Fig. 1A**). *Pexa-Vec*–related grade 3 and 4 adverse events included lymphopenia and neutropenia (Supplementary Table S1). Patient 09 experienced grade 4 intraoperative hypotension that was regarded to be unrelated to *Pexa-Vec*. Surgery was undertaken in all but 1 patient (patient 07), where plans for surgery were abandoned after finding pulmonary metastases on an up-to-date preoperative CT scan. At the time of writing, after more than 3 years of follow-up post–*Pexa-Vec* infusion for each patient, 5 of the 9 patients were alive. The 3 patients that remained cancer-free all had CRLM (patients 05, 06, and 08). Pathologic examination of their resected tumor specimens post–*Pexa-Vec* infusion revealed extensive (patient 05) or complete (patient 08) necrosis of the tumor in 2 of the 3 patients (**Fig. 1B**; Supplementary Table S1). None of the other resected patient tumors showed any signs of necrosis.

### Intravenous *Pexa-Vec* associates with plasma, but not PBMCs

In contrast to our previous clinical trial findings using intravenous reovirus infusions (29, 30), qPCR analysis of peripheral blood compartments revealed that *Pexa-Vec* associated with plasma, but not PBMCs (**Table 1**), being detectable at 1 hour postinfusion in 4 of the 9 patients. This was confirmed in *Pexa-Vec*–pulsed blood, donated from healthy volunteers, where *Pexa-Vec* could only be detected in the separated plasma fraction (**Fig. 1C**). However, in patient 05, extensive tumor necrosis was noted following *Pexa-Vec* infusion (Supplementary Table S1), and qPCR of plasma only revealed the presence of virus immediately presurgery [22 days postinfusion (**Table 1**)]. This potentially signified ongoing virus production from the tumor at this time point. In common with reovirus infusion (30), *Pexa-Vec* neutralizing antibodies peaked either at the time of surgery or 1-month post-surgery (**Fig. 1D**).

Intravenous *Pexa-Vec* infects CRLM

IHC analysis of four of five resected CRLMs revealed the presence of *Pexa-Vec* protein in the tumors from patients 02 and 09, on the periphery of the tumor from patient 08, and its absence from the tumor of patient 06 (**Fig. 2A**). The available tissue from patient 05′s tumor could not be assessed due to tissue necrosis. To confirm the specificity of *Pexa-Vec* to CRLM compared with the surrounding liver, we treated *ex vivo* tissue core biopsy samples from patients undergoing standard CRLM surgical resections outside the trial with *Pexa-Vec*. At 96 hours posttreatment, large areas of CRLM core biopsies were infected with *Pexa-Vec*, as determined by immunofluorescence for virus-expressed GFP (**Fig. 2B**). In contrast, separate core biopsies taken from background livers were resistant to *Pexa-Vec* infection, with GFP only detected in scattered cells, indicating nonproductive infection (**Fig. 2B**).

Pexa-Vec stimulates anticancer NK-cell activity

A total of 24 hours after *Pexa-Vec* infusion, a significant increase in plasma IFNα concentrations (**Fig. 3A**; Supplementary Table S2), in addition to other proinflammatory, proapoptotic, and DC maturation-associated cytokines such as IL12, TNF-related apoptosis-inducing ligand (TRAIL), and lysosome-associated membrane glycoprotein 3 (LAMP3), respectively (Supplementary Fig. S1A and S1B; Supplementary Table S2; ref. 31). Gene expression of a panel of IFN-stimulated
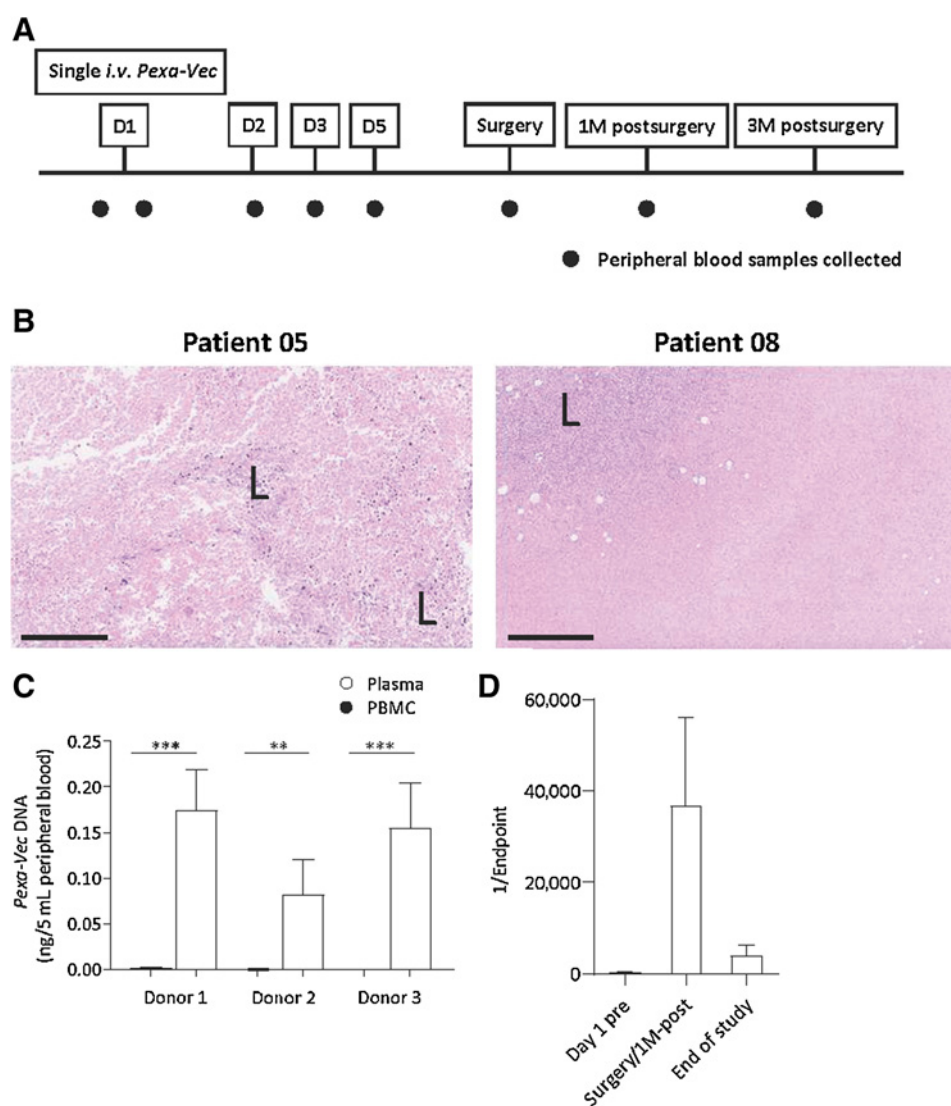
Figure 1.
Pexa-Vec peripheral blood carriage. **A,** Trial schema showing the timing [day (D); month (M)] of *Pexa-Vec* infusion and collection of translational blood samples. **B,** H&E staining of tumor sections from patients 05 and 08 showing areas of necrosis. "L" indicates lymphocytic infiltrate. Bars, 400 μm. **C,** qPCR quantification of *Pexa-Vec* in the plasma or PBMCs of three healthy donors following *ex vivo* addition of virus to whole blood. Data are shown as mean + SEM ng DNA in PBMCs or plasma extracted from an initial 5 mL peripheral blood. **, $P < 0.01$; ***, $P < 0.001$ by unpaired t tests; $n = 9$. **D,** Neutralizing antibodies to *Pexa-Vec* in patient serum following intravenous infusion. Plot shows mean + SEM previrus, peak at surgery/1M after and end of study titers in $n = 9$ patients.

genes (ISG) significantly increased in PBMCs 24 hours post–*Pexa-Vec* (**Fig. 3B**). Inflammatory cytokine protein and RNA expression gradually reduced to baseline levels by the time of surgery (**Fig. 3A** and **B**; Supplementary Fig. S1A and S1B; Supplementary Table S2).

**Table 1.** qPCR analysis for the presence of *Pexa-Vec* in patient PBMCs or plasma at all time points.

Patient	PBMC qPCR	Plasma qPCR
01	−	−
02	−	+ (1 hour post)
03	−	+ (1 hour post)
04	−	+ (1 hour post)
05	−	+ (surgery)
06	−	−
07	−	−
08	−	−
09	−	+ (1 hour post)

Note: "+" and "−" indicate positive and negative detection, respectively.

Given that NK cells are activated by ISGs, including IL12 (32), we measured patient-derived peripheral blood NK-cell activation and cytolytic activity against tumor-relevant cell line targets. We found significantly increased NK-cell activation, as measured by CD69 expression, on days 2 and 3, with a reduction to baseline levels by day 5 [**Fig. 3**C(i); Supplementary Fig. S2A]. NK-cell cytolytic activity was significantly increased 24 hours following *Pexa-Vec* infusion, before decreasing to baseline at day 5 [**Fig. 3**C(ii); Supplementary Fig. S2B]. In common with other oncolytic viruses (29, 33), the critical role of IFNα/β in NK-cell activation following *Pexa-Vec* stimulation was confirmed by simultaneous blockade of the type I IFN receptor and of soluble IFNα/β within *in vitro Pexa-Vec*–treated PBMCs. This resulted in a significant reduction in NK-cell activation, as assessed by cell surface CD69 expression and cytolytic activity (**Fig. 3D**). Previous work indicates that monocytes are the source of both oncolytic reovirus and herpes simplex virus-induced type I IFNs (34, 35). We confirmed a critical role for monocytes in mediating NK activity following *Pexa-Vec* stimulation, whereby depletion of monocytes from PBMCs significantly reduced NK-cell activation and function (**Fig. 3E**).

Figure 2.
Pexa-Vec detection in resected CRLM specimens. **A,** The presence of *Pexa-Vec* in surgical tissue was assessed by IHC following intravenous infusion. Representative slides from 4 patients shows vaccinia protein (brown), secondary antibody-alone controls (2 Ab), and H&E stains in consecutive sections. **B,** Tissue core biopsies taken from resected CRLM and background liver samples from patients undergoing standard surgery outside the clinical trial. Patient samples were treated with *Pexa-Vec*-GFP or PBS prior to confocal fluorescent imaging. Images shown are for 1 of 10 representative patients. All bars indicate 200 μm.
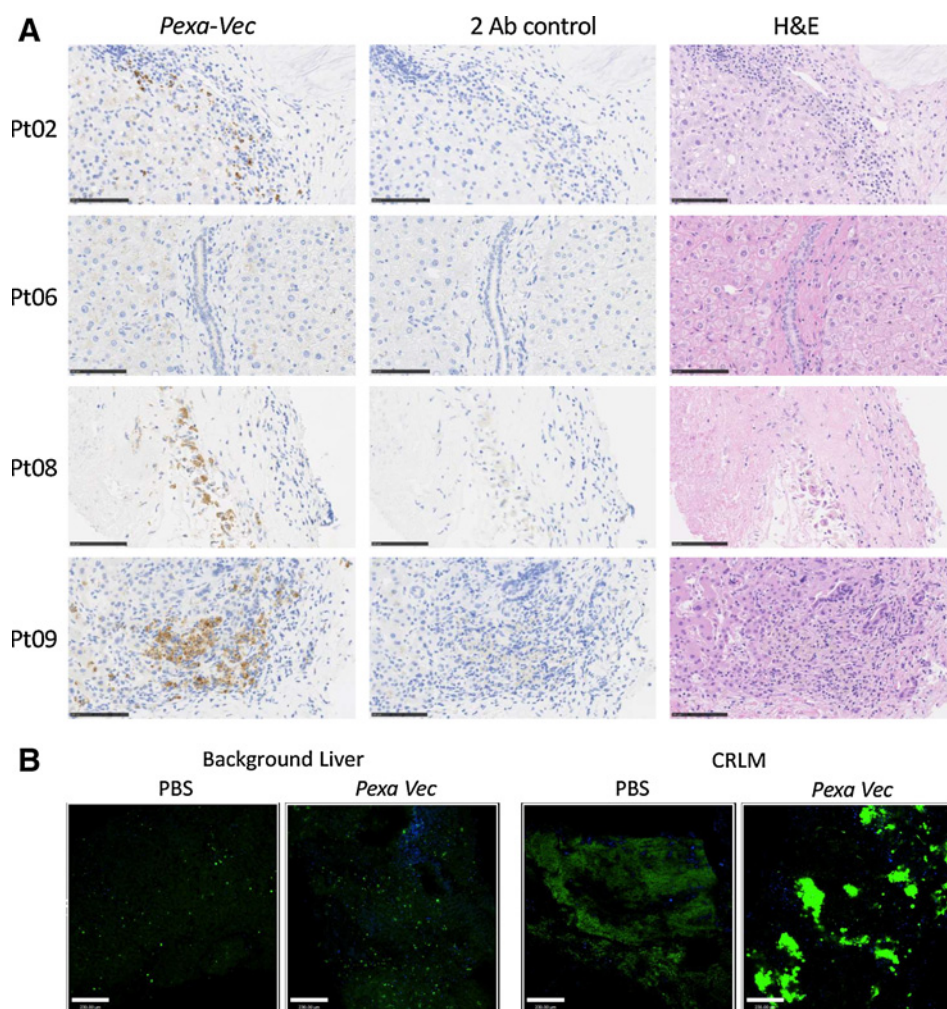
Because IFNs stimulate upregulation of programmed death protein 1 (PD-1) (29), we analyzed expression of this immunosuppressive immune checkpoint in patient 01, comparing the pre–*Pexa-Vec* tumor biopsy with the resected tumor sample. In keeping with the observed induction of ISGs, we found more concentrated PD-1 staining post-*Pexa Vec* infusion (Supplementary Fig. S3A). PD-1–expressing cells lacked Ki67 staining, confirming that they were nonreplicating and likely to be immunologically exhausted. Examination of post-*Pexa Vec* tumor samples from other patients on study similarly revealed areas of PD-1–expressing nonreplicating cells (Supplementary Fig. S3B).

Chemokine induction

Pexa-Vec infusion was followed by a reduction in the peripheral lymphocyte concentration in all patients at day 2, returning to baseline levels by the time of surgery (**Fig. 4A**). We confirmed that this was unlikely due to lymphocyte cell death in an *in vitro* cell viability assay (**Fig. 4B**). *Pexa-Vec* also associated with *CXCL10* gene expression in PBMCs and a corresponding peak in plasma CXCL10 (also known as IFNγ-induced protein 10; IP-10) protein levels 24 hours following virus infusion (**Fig. 4C**; Supplementary Table S3). IP-10 is a chemokine known to play an important role in recruiting activated T cells into sites of tissue inflammation and associates with the presence of CD8$^+$ T cells in tumors (36, 37). Concordantly, the observed kinetics of peripheral blood lymphopenia closely followed the rise and fall

in IP-10 concentrations and *CXCL10* gene expression. On examination, all resected tumors harbored infiltrating CD8$^+$ T cells (**Fig. 4D**). CD8$^+$ T cells were frequently associated with malignant cells, as exemplified by the resected lymph node from patient 04, where CD8$^+$ T cells were found in higher concentrations in association with melanoma cell clusters (Supplementary Fig. S4A) than in areas of the same lymph node with few infiltrating melanoma cells. In patient 01, where a pre–*Pexa-Vec* tumor biopsy was available, comparison with the resected tumor sample post–*Pexa-Vec* revealed a shift in the CD8$^+$ T-cell population, from a perivascular localization at baseline to a wider infiltrative distribution across the tumor postvirus infusion (Supplementary Fig. S4B). In addition to increased *CXCL10*, gene expression of *CCL2*, a chemotactic cytokine that induces directional migration of DCs into infected tissue, also peaked at day 2 and returned to baseline by the time of surgery (Supplementary Fig. S5; ref. 38).

Pexa-Vec stimulates functional anticancer T-cell activity

In addition to the observed innate anticancer immune effects, successful anticancer therapy requires a longer-lived T-cell immune response. We therefore measured the effects of *Pexa-Vec* infusion on functional T-cell responses via PBMC IFNγ secretion using ELISpot assays. Patient-derived PBMCs were stimulated *ex vivo* using overlapping peptide pools of TAAs, either MART-1 for PBMCs derived from patients with melanoma or CEA for PBMCs isolated from
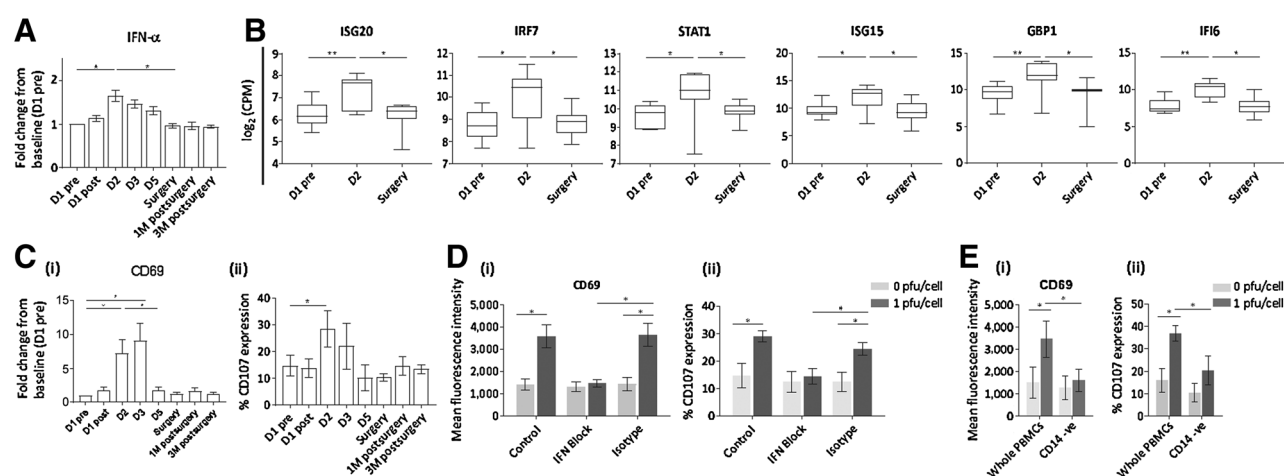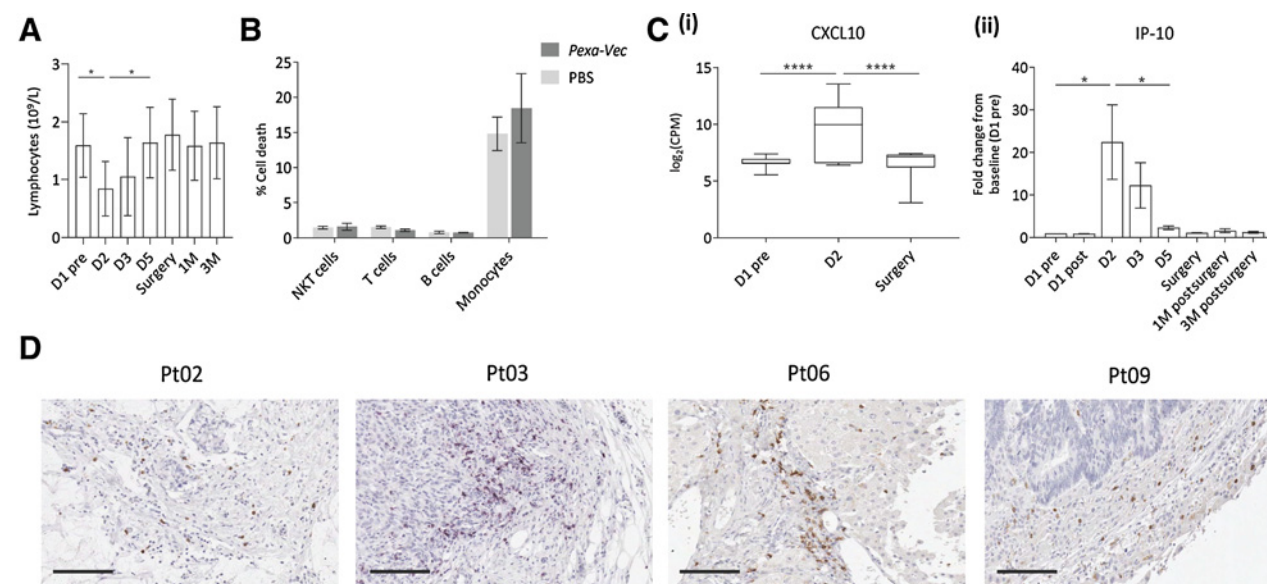
Figure 3.
Innate immune response to *Pexa-Vec*. **A,** Peripheral blood plasma IFNα concentration following *Pexa-Vec* infusion was determined by multiplex analysis. Data are shown as fold change from baseline [day (D)1 pre] samples. *, $P < 0.05$ by paired t tests; $n = 4$. **B,** Differential ISG expression analysis of mRNA isolated from CRLM trial patient PBMCs at D1 pre, D2, and surgery. Data are expressed as $\log_2$ (CPM). P_{adj} value was determined after using the Benjamini and Hochberg (1995) method for controlling the FDR; *, $P < 0.05$; **, $P < 0.01$; $n = 6$. **C,** Patient PBMCs were collected at the indicated time points. Patient NK-cell activation was determined via (i) CD69 expression and (ii) NK degranulation against Mel888 cells (for patients with melanoma) or SW620 cells (for patients with CRLM) and shown as percent positive CD107 expression. *, $P < 0.05$ by paired t tests; $n = 9$ for both. **D,** NK-cell activation (CD69 expression) (i) and NK degranulation (ii) of healthy donor PBMCs following stimulation with *Pexa-Vec* in the presence of IFNα/β blockade or isotype control. *, $P < 0.05$ by unpaired t tests; $n = 4$. **E,** NK-cell activation (i) and degranulation (ii) of healthy donor PBMCs ± monocyte depletion (CD14⁻) prior to stimulation with *Pexa-Vec*. *, $P < 0.05$ by unpaired t tests; $n = 4$. All data are shown as mean ± SEM.

patients with CRLM, which were confirmed to be expressed in the corresponding tumor samples (**Fig. 5A**). Although very few MART-1 or CEA–specific IFNγ-producing cells were observed at baseline pre–*Pexa-Vec*, this increased following *Pexa-Vec* infusion (**Fig. 5B**). A similar increase was seen in IFNγ-producing cells specific to CEF (cytomegalovirus, Epstein–Barr virus, influenza virus) over-

lapping peptide pools, which were used as a positive control (Supplementary Fig. S6A). T-cell responses to either CEA and MART-1 for all patients peaked at 1-month postsurgery and remained elevated over pre–*Pexa-Vec* baseline levels (**Fig. 5C**; Supplementary Fig. S6B). T-cell responses remained elevated at least 3 months following *Pexa-Vec* infusion, indicating the

Figure 4.
Chemokine expression and CD8⁺ T-cell tumor infiltration. **A,** Trial patient peripheral blood lymphocyte concentrations prior to [day (D)1 pre] and post–*Pexa-Vec* infusion [M: month(s)]. *, $P < 0.05$ by paired t test; $n = 9$. **B,** Cell death of healthy donor PBMC populations treated with *Pexa-Vec* or PBS ($n = 3$). **C,** *Pexa-Vec*–treated trial patient PBMCs were assessed for (i) mRNA expression of *CXCL10*. P_{adj} value was determined after using the Benjamini and Hochberg method for controlling FDR; ****, $P < 0.0001$; $n = 7$. (ii) Multiplex quantification of CXCL10 protein (IP-10) in trial patient plasma. *, $P < 0.05$ by paired t tests; $n = 9$. All data are shown as mean ± SEM. **D,** IHC staining (brown) of CD8-expressing cells within representative trial patient tumors following *Pexa-Vec* infusion. Bars, 100 μm.

Figure 5.
T-cell functional anticancer responses. **A,** Representative IHC of patient tumors showing MART-1 (patient 01) and CEA (patient 05) expression (purple and brown, respectively), with corresponding secondary antibody controls (2 Ab). Bars, 200 μm. **B,** Representative ELISpot images from patients 01 and 05 at the indicated time points. PBMCs were stimulated using MART-1 and CEA overlapping peptide pools, respectively. Duplicate wells are shown for each time point. Data are shown as SFU per well; each spot represents an IFNγ-secreting T cell. **C,** Cumulative CEA and MART-1 IFNγ responses from all 9 patients via ELISpot. Data are shown as mean + SEM SFU/well. *, $P < 0.05$ by paired t tests; $n = 7$–9, depending on sample availability. **D,** Estimated numbers of CD8 T cells that belong to specific MART-1 TAA clones. Data shown for melanoma patients 01, 03, and 04.

induction of long-lived T-cell anticancer immune responses (**Fig. 5C**). We confirmed these findings for MART-1 and other TAAs by T-cell receptor (TCR) sequencing using DNA derived from trial patient PBMCs at baseline, surgery, and at the end of study. Examination of the relative numbers of individual T-cell clones was performed against published databases of TCR epitope specificity [VDJdb (39), PIRD (40), and McPAS-TCR (41)], where these data were available. Analysis revealed clonal proliferation of MHC class I–restricted (CD8) T cells following *Pexa-Vec* infusion, targeting MART-1 (**Fig. 5D**; Supplementary Table S4) and other TAAs (Supplementary Table S4).

Reduced T-cell clonal diversity associates with pathologic tumor response

Despite the observed NK-cell cytolytic activity and the functional T-cell anticancer immune responses across all the trial patients, tumor necrosis was only observed in the CRLM of patients 05 and 08. We, therefore, characterized changes in peripheral blood T-cell clonal evolution in the 9 trial patients to elucidate whether this could be a determining factor for the observed differences in tumor necrosis. Longitudinal analysis of these data showed changes in the V-J TCR usage, which are displayed as circos plots (**Fig. 6A**) where the width of each band is proportional to the frequency of usage of that gene segment. Individual gene regions were labeled, and a

transient increase in the use of TRBV20-1 was seen in the 2 patients who displayed tumor necrosis (patient 05 and 08), along with a similar increase in TCRBV18 in the patient displaying complete necrosis (patient 08). This was in contrast to a more stable gene family usage profile exhibited by other patients with no visible necrosis, as exemplified by patient 06. The small patient numbers involved limited statistical inference; however, increased usage of TRBV18 and TRBV20-1 draws parallels with a prior study examining tumor-infiltrating lymphocytes within colorectal cancer biopsies and may indicate a TAA-driven T-cell response (42).

Tracking changes in the abundance of T-cell clones following *Pexa-Vec* infusion revealed that by the time of surgery, there was a reduction in the diversity of the most highly abundant T-cell clones derived from patients 05 and 08 compared with other patients, as estimated by the inverse Simpson index (**Fig. 6B**). Statistical analysis revealed that this drop in T-cell diversity for patients 05 and 08 was significant ($P = 0.036$) compared with the other patients that had no tumor necrosis at the time of surgery (**Fig. 6C**). We investigated whether this could be due to differences in T-cell responses to *Pexa-Vec*. Comparison of longitudinal PBMC IFNγ production via ELISpot between patients 05 (extensive tumor necrosis) and 06 (no tumor necrosis) revealed an expected increase in responses at the time of surgery, which reduced at the end of study but showed no discernible difference between the 2 patients (Supplementary Fig. S7). Therefore, CRLM necrosis

Figure 6.
TCR sequencing of trial patient PBMCs. **A,** Circos plots showing the association of V-gene (lower half of plot) and J-gene (upper half of plot) segments at different time points for patients 05, 06, and 08. Width of the ribbon is indicative of the relative usage of each segment at each time point. **B,** Percent change in TCR diversity as calculated by inverse Simpson index. **C,** Percent change in the diversity of T-cell clones at surgery to compare patients with defined necrosis and patients with no tumor necrosis. *, $P < 0.05$ by one-tailed Mann–Whitney test ($n = 8$). Data are shown as mean $\pm$ SEM.

in patients 05 and 08 following *Pexa-Vec* infusion appeared to be associated with a reduction in the diversity of the most highly proliferated T-cell clones. This observation could, in part, be accounted for by proliferation of select TRBV18 and TRBV20-1 T-cell clonotypes targeting TAAs, in contrast to a more diverse naïve $CD8^+$ TCR repertoire in patients without tumor necrosis. This is reminiscent of the same observation in patients with melanoma who experienced durable progression-free survival following treatment with a neoantigen vaccine and PD-1 inhibition (43). In these patients, the presence of increased effector memory $CD8^+$ T cells was reflected by a more restricted and less diverse circulating TCR repertoire than in patients who experienced progressive disease.

Discussion and Conclusions

Our results showed that neoadjuvant intravenous *Pexa-Vec* therapy is well tolerated in patients with metastatic melanoma and CRLM, has tumor-specific replication, and shows evidence of clinical efficacy, including pathologic tumor response. *Pexa-Vec* was detected in three of the four available CRLM specimens, confirming previous findings of intravenous delivery of *Pexa-Vec* to tumors when using the same or higher doses (14). In contrast to our previous findings of the cellular carriage of oncolytic reovirus to tumors following intravenous infusion (29, 30), intravenous *Pexa-Vec* administration resulted in plasma-based carriage, with no association of virus with PBMCs. The development of neutralizing antibodies to *Pexa-Vec* at the time of surgery is consistent with the timing of seroconversion previously reported for *Pexa-Vec*, as well as for other intravenously administered oncolytic viruses (44, 45). In contrast to oncolytic reovirus, which is delivered to tumors by peripheral blood cell carriage (46), and results in the shielding of virus from antibody neutralization (47), the development of *Pexa-Vec* antibodies will likely hinder intravenous delivery from that time point onward (48). Strategies to reduce antibody neutralization are being tested clinically for other oncolytic poxviruses, including TG6002, an engineered Copenhagen strain vaccinia virus under clinical development by Transgene, which is being delivered by

hepatic artery infusion in patients with CRLM (ClinicalTrials.gov Identifier: NCT04194034).

Our study characterizes the innate and adaptive immune response to intravenous *Pexa-Vec* infusion in patients with cancer. In accordance with results from other oncolytic virus clinical trials, *Pexa-Vec* administration stimulated IFN expression, which peaked 24 hours after infusion (49, 50). This resulted in a broad inflammatory cytokine and chemokine response, despite the potential for immunosuppressive vaccinia virus gene expression of encoding proteins that act as decoy receptors to block the activity of type I IFNs (51). The expressed cytokines associated with NK-cell activation and the proliferation of $CD8^+$ T-cell clones specific for TAAs, despite the presence of exhausted cell populations. The correlation seen between pathological tumor response and reduction in peripheral TCR diversity requires confirmation in larger trials. Although we have not, within the confines of the current study, specified the nature of these T-cell populations, we suggest that pathologic tumor response is driven by a proliferative, low diversity clonal T-cell population targeting TAAs. If confirmed in a larger study, our results would support a strategy to encode selected HLA-matched tumor-specific epitopes within oncolytic viruses, or non–HLA-specific TAAs, instead of the pursuit of broad-spectrum, low-level T-cell stimulation.

Disappointing phase III results using *Pexa Vec* in combination with sorafenib in advanced hepatocellular carcinoma (NCT02562755) indicate the need to better rationalize combinations and schedules of therapy. Despite the size of the present study and heterogeneity of the tumor cohort, our findings, in conjunction with the excellent safety data from our previous neoadjuvant oncolytic virus studies (29, 30), supports the development of this class of immunotherapies toward standard clinical practice in the neoadjuvant setting. Rational combinations with nonoverlapping toxicities are needed to increase efficacy. The most promising oncolytic virus combination is with the targeting of immune checkpoint proteins, which are frequently upregulated in the presence of both pathogenic and therapeutic viral infections (29, 52–54), and act to dampen $CD8^+$ T-cell responses. The

sequential combination of an oncolytic virus followed by PD-1 or PD-L1 blockade has produced remarkable results in preclinical models (29, 54) and is currently being tested in numerous early- (55) and late-phase (ClinicalTrials.gov Identifier: NCT02263508) clinical trials for a wide variety of malignancies. Likewise, tumor-conditioning using intratumoral *Pexa-Vec* followed by PD-1 blockade is currently being tested in patients with advanced hepatocellular carcinoma (Clinical-Trials.gov Identifier: NCT03071094). To aid in the clinical progression of oncolytic vaccinia therapy, further research should seek reliable baseline biomarkers that predict tumor response and clinical prognosis following virus treatment, in conjunction with the associated clinical disease parameters.

Authors' Disclosures

Authors' Contributions

A. Samson: Conceptualization, data curation, formal analysis, supervision, funding acquisition, writing–original draft, writing–review and editing. **E.J. West:** Conceptualization, formal analysis, validation, investigation, methodology, writing–original draft, writing–review and editing. **J. Carmichael:** Formal analysis, methodology. **K.J. Scott:** Formal analysis, investigation, methodology, writing–original draft, writing–review and editing. **S. Turnbull:** Enrolment of patients. **B. Kuszlewicz:** Formal analysis, methodology. **R.V. Dave:** Methodology. **A. Peckham-Cooper:** Methodology. **E. Tidswell:** Methodology. **J. Kingston:** Methodology. **M. Johnpulle:** Methodology. **B. da Silva:** Methodology. **V.A. Jennings:** Methodology. **K. Bendjama:** Conceptualization, methodology. **N. Stojkowitz:** Conceptualization. **M. Lusky:** Conceptualization. **K.R. Prasad:** Patient management. **G.J. Toogood:** Patient management. **R. Auer:** Conceptualization. **J. Bell:** Conceptualization. **C.J. Twelves:** Conceptualization, management of patients. **K.J. Harrington:** Writing–original draft. **R.G. Vile:** Writing–original draft. **H. Pandha:** Writing–original draft. **F. Errington-Mais:** Conceptualization, writing–original draft. **C. Ralph:** Conceptualization. **D.J. Newton:** Conceptualization, writing–original draft. **A. Anthoney:** Patient management. **A.A. Melcher:** Conceptualization, writing–original draft. **F. Collinson:** Conceptualization.

Acknowledgments

References

1. Nordlinger B, Sorbye H, Glimelius B, Poston GJ, Schlag PM, Rougier P, et al. Perioperative FOLFOX4 chemotherapy and surgery versus surgery alone for resectable liver metastases from colorectal cancer (EORTC 40983): long-term results of a randomised, controlled, phase 3 trial. Lancet Oncol 2013;14:1208–15.
2. Eggermont AMM, Chiarion-Sileni V, Grob J-J, Dummer R, Wolchok JD, Schmidt H, et al. Prolonged survival in stage III melanoma with ipilimumab adjuvant therapy. N Engl J Med 2016;375:1845–55.
3. Russell L, Peng K-W. The emerging role of oncolytic virus therapy against cancer. Chinese Clin Oncol 2018;7:16.
4. Kim JH, Oh JY, Park BH, Lee DE, Kim JS, Park HE, et al. Systemic armed oncolytic and immunologic therapy for cancer with JX-594, a targeted poxvirus expressing GM-CSF. Mol Ther 2006;14:361–70.
5. Transgene. Jennerex and transgene enter into an exclusive partnership for the development and commercialization of JX-594 for the treatment of cancers; 2010. Available from: http://www.transgene.fr/index.php?option=com_press_release&task=download&id=172&l=en.
6. Transgene. Transgene supports proposed acquisition of Jennerex by SillaJen; 2013. Available from: http://www.transgene.fr/index.php?option=com_press_release&task=download&id=243&l=en.
7. Hengstschläger M, Pfeilstöcker M, Wawra E. Thymidine kinase expression. A marker for malignant cells. Adv Exp Med Biol 1998;431:455–60.
8. Urdinguio RG, Fernandez AF, Moncada-Pazos A, Huidobro C, Rodriguez RM, Ferrero C, et al. Immune-dependent and independent antitumor activity of GM-CSF aberrantly expressed by mouse and human colorectal tumors. Cancer Res 2013;73:395–405.
9. Mach N, Gillessen S, Wilson SB, Sheehan C, Mihm M, Dranoff G. Differences in dendritic cells stimulated *in vivo* by tumors engineered to secrete granulocyte-macrophage colony-stimulating factor or Flt3-ligand. Cancer Res 2000;60:3239–46.
10. Kirn D. Systemic treatment of metastatic and/or systemically-disseminated cancers using gm-csf-expressing poxviruses WO 2007030668 A3; 2006.
11. Kim MK, Breitbach CJ, Moon A, Heo J, Lee YK, Cho M, et al. Oncolytic and immunotherapeutic vaccinia induces antibody-mediated complement-dependent cancer cell lysis in humans. Sci Transl Med 2013;5:185ra63.
12. Breitbach CJ, Arulanandam R, De Silva N, Thorne SH, Patt R, Daneshmand M, et al. Oncolytic vaccinia virus disrupts tumor-associated vasculature in humans. Cancer Res 2013;73:1265–75.
13. Heo J, Breitbach C, Cho M, Hwang T-H, Kim CW, Jeon UB, et al. Phase II trial of Pexa-Vec (pexastimogene devacirepvec; JX-594), an oncolytic and immunotherapeutic vaccinia virus, followed by sorafenib in patients with advanced hepatocellular carcinoma (HCC). J Clin Oncol 31: 15s, 2013 (suppl; abstr 4122).
14. Breitbach CJ, Burke J, Jonker D, Stephenson J, Haas AR, Chow LQM, et al. Intravenous delivery of a multi-mechanistic cancer-targeted oncolytic poxvirus in humans. Nature 2011;477:99–102.
15. Wurdak H, Zhu S, Romero A, Lorger M, Watson J, Chiang C-Y, et al. An RNAi screen identifies TRRAP as a regulator of brain tumor-initiating cell differentiation. Cell Stem Cell 2010;6:37–47.
16. White CL, Twigger KR, Vidal L, De Bono JS, Coffey M, Heinemann L, et al. Characterization of the adaptive and innate immune response to intravenous oncolytic reovirus (Dearing type 3) during a phase I clinical trial. Gene Ther 2008;15:911–20.
17. Van Dongen JJM, Langerak AW, Brüggemann M, Evans PAS, Hummel M, Lavender FL, et al. Design and standardization of PCR primers and protocols for detection of clonal immunoglobulin and T-cell receptor gene recombinations in suspect lymphoproliferations: Report of the BIOMED-2 concerted action BMH4-CT98-3936. Leukemia 2003;17:2257–317.

18. Andrews S. FastQC: A quality control tool for high throughput sequence data. Available from: http://www.bioinformatics.babraham.ac.uk/projects/fastqc/.

19. Bolger AM, Lohse M, Usadel B. Trimmomatic: a flexible trimmer for Illumina sequence data. Bioinformatics 2014;30:2114–20.

20. Babraham Bioinformatics. Trim Galore, Version 0.6.5; 2019. Available from: https://www.bioinformatics.babraham.ac.uk/projects/trim_galore/.

21. Magoč T, Salzberg SL. FLASH: fast length adjustment of short reads to improve genome assemblies. Bioinformatics 2011;27:2957–63.

22. Bolotin DA, Poslavsky S, Mitrophanov I, Shugay M, Mamedov IZ, Putintseva EV, et al. MiXCR: Software for comprehensive adaptive immunity profiling. Nat Methods 2015;12:380–1.

23. Shugay M, Bagaev DV, Turchaninova MA, Bolotin DA, Britanova OV, Putintseva EV, et al. VDJtools: Unifying post-analysis of T cell receptor repertoires. PLOS Comput Biol 2015;11:e1004503.

24. Team RC. The R Project for statistical computing; 2014.

25. Team ImmunoMind. immunarch: An R package for painless analysis of large-scale immune repertoire data; 2019.

26. Gu Z, Gu L, Eils R, Schlesner M, Brors B. circlize implements and enhances circular visualization in R. Bioinformatics 2014;30:2811–2.

27. Wickham H. Ggplot2: Elegant graphics for data analysis. New York: Springer-Verlag; 2016.

28. Adair RA, Scott KJ, Fraser S, Errington-Mais F, Pandha H, Coffey M, et al. Cytotoxic and immune-mediated killing of human colorectal cancer by reovirus-loaded blood and liver mononuclear cells. Int J Cancer 2013;132:2327–38.

29. Samson A, Scott KJ, Taggart D, West EJ, Wilson E, Nuovo GJ, et al. Intravenous delivery of oncolytic reovirus to brain tumor patients immunologically primes for subsequent checkpoint blockade. Sci Transl Med 2018;10:eaam7577.

30. Adair RA, Roulstone V, Scott KJ, Morgan R, Nuovo GJ, Fuller M, et al. Cell carriage, delivery, and selective replication of an oncolytic virus in tumor in patients. Sci Transl Med 2012;4:138ra77.

31. Korthals M, Safaian N, Kronenwett R, Maihöfer D, Schott M, Papewalis C, et al. Monocyte derived dendritic cells generated by IFN-α acquire mature dendritic and natural killer cell properties as shown by gene expression analysis. J Transl Med 2007;5:46.

32. Tripp CS, Wolf SF, Unanue ER. Interleukin 12 and tumor necrosis factor alpha are costimulators of interferon gamma production by natural killer cells in severe combined immunodeficiency mice with listeriosis, and interleukin 10 is a physiologic antagonist. Proc Natl Acad Sci U S A 1993;90:3725–9.

33. Müller LME, Holmes M, Michael JL, Scott GB, West EJ, Scott KJ, et al. Plasmacytoid dendritic cells orchestrate innate and adaptive anti-tumor immunity induced by oncolytic coxsackievirus A21. J Immunother Cancer 2019;7:164.

34. Jennings VA, Scott GB, Rose AMS, Scott KJ, Migneco G, Keller B, et al. Potentiating oncolytic virus-induced immune-mediated tumor cell killing using histone deacetylase inhibition. Mol Ther 2019;27:1139–52.

35. Parrish C, Scott GB, Migneco G, Scott KJ, Steele LP, Ilett E, et al. Oncolytic reovirus enhances rituximab-mediated antibody-dependent cellular cytotoxicity against chronic lymphocytic leukaemia. Leukemia 2015;29:1799–810.

36. Dufour JH, Dziejman M, Liu MT, Leung JH, Lane TE, Luster AD. IFN-gamma-inducible protein 10 (IP-10; CXCL10)-deficient mice reveal a role for IP-10 in effector T cell generation and trafficking. J Immunol 2002;168:3195–204.

37. Harlin H, Meng Y, Peterson AC, Zha Y, Tretiakova M, Slingluff C, et al. Chemokine expression in melanoma metastases associated with CD8 + T-CeII recruitment. Cancer Res 2009;69:3077–85.

38. Xu LL, Warren MK, Rose WL, Gong W, Wang JM. Human recombinant monocyte chemotactic protein and other c-c chemokines bind and induce directional migration of dendritic cells in vitro. J Leukoc Biol 1996;60:365–71.

39. Bagaev DV, Vroomans RMA, Samir J, Stervbo U, Rius C, Dolton G, et al. VDJdb in 2019: database extension, new analysis infrastructure and a T-cell receptor motif compendium. Nucleic Acids Res 2020;48:D1057–62.

40. Zhang W, Wang L, Liu K, Wei X, Yang K, Du W, et al. PIRD: pan immune repertoire database. Bioinformatics 2020;36:897–903.

41. Tickotsky N, Sagiv T, Prilusky J, Shifrut E, Friedman N. McPAS-TCR: a manually curated catalogue of pathology-associated T cell receptor sequences. Bioinformatics 2017;33:2924–9.

42. Sherwood AM, Emerson RO, Scherer D, Habermann N, Buck K, Staffa J, et al. Tumor-infiltrating lymphocytes in colorectal tumors display a diversity of T cell receptor sequences that differ from the T cells in adjacent mucosal tissue. Cancer Immunol Immunother 2013;62:1453–61.

43. Ott PA, Hu-Lieskovan S, Chmielowski B, Govindan R, Naing A, Bhardwaj N, et al. A phase Ib trial of personalized neoantigen therapy plus anti-PD-1 in patients with advanced melanoma, non-small cell lung cancer, or bladder cancer. Cell 2020;183:347–62.

44. Hwang T-H, Moon A, Burke J, Ribas A, Stephenson J, Breitbach CJ, et al. A mechanistic proof-of-concept clinical trial with JX-594, a targeted multi-mechanistic oncolytic poxvirus, in patients with metastatic melanoma. Mol Ther 2011;19:1913–22.

45. Machiels J-P, Salazar R, Rottey S, Duran I, Dirix L, Geboes K, et al. A phase 1 dose escalation study of the oncolytic adenovirus enadenotucirev, administered intravenously to patients with epithelial solid tumors (EVOLVE). J Immunother Cancer 2019;7:20.

46. Ilett EJ, Bárcena M, Errington-Mais F, Griffin S, Harrington KJ, Pandha HS, et al. Internalization of oncolytic reovirus by human dendritic cell carriers protects the virus from neutralization. Clin Cancer Res 2011;17:2767–76.

47. Berkeley RA, Steele LP, Mulder AA, Van Den Wollenberg DJM, Kottke TJ, Thompson J, et al. Antibody-neutralized reovirus is effective in oncolytic virotherapy. Cancer Immunol Res 2018;6:1161–73.

48. Panchanathan V, Chaudhri G, Karupiah G. Protective immunity against secondary poxvirus infection is dependent on antibody but not on CD4 or CD8 T-cell function. J Virol 2006;80:6333–8.

49. Guillerme J-B, Boisgerault N, Roulois D, Ménager J, Combredet C, Tangy F, et al. Measles virus vaccine-infected tumor cells induce tumor antigen cross-presentation by human plasmacytoid dendritic cells. Clin Cancer Res 2013; 19:1147–58.

50. Benencia F, Courrèges MC, Conejo-García JR, Mohamed-Hadley A, Zhang L, Buckanovich RJ, et al. HSV oncolytic therapy upregulates interferon-inducible chemokines and recruits immune effector cells in ovarian cancer. Mol Ther 2005; 12:789–802.

51. Perdiguero B, Esteban M. The interferon system and vaccinia virus evasion mechanisms. J Interferon Cytokine Res 2009;29:581–98.

52. Golden-Mason L, Palmer B, Klarquist J, Mengshol JA, Castelblanco N, Rosen HR. Upregulation of PD-1 expression on circulating and intrahepatic hepatitis C virus-specific CD8+ T cells associated with reversible immune dysfunction. J Virol 2007;81:9249–58.

53. Ribas A, Dummer R, Puzanov I, Vanderwalde A, Andtbacka RHI, Michielin O, et al. Oncolytic virotherapy promotes intratumoral T cell infiltration and improves anti-PD-1 immunotherapy. Cell 2017;170:1109–19.

54. Bourgeois-Daigneault M-C, Roy DG, Aitken AS, El Sayes N, Martin NT, Varette O, et al. Neoadjuvant oncolytic virotherapy before surgery sensitizes triple-negative breast cancer to immune checkpoint therapy. Sci Transl Med 2018;10: eaao1641.

55. Larocca CJ, Warner SG. Oncolytic viruses and checkpoint inhibitors: combination therapy in clinical trials. Clin Transl Med 2018;7:35.